

Supplementary information

Enhanced Photochemical Activity and Ultrafast Photocarrier Dynamics in Sustainable Synthetic Melanin Nanoparticle-Based Donor-Acceptor Inkjet-Printed Molecular Junctions

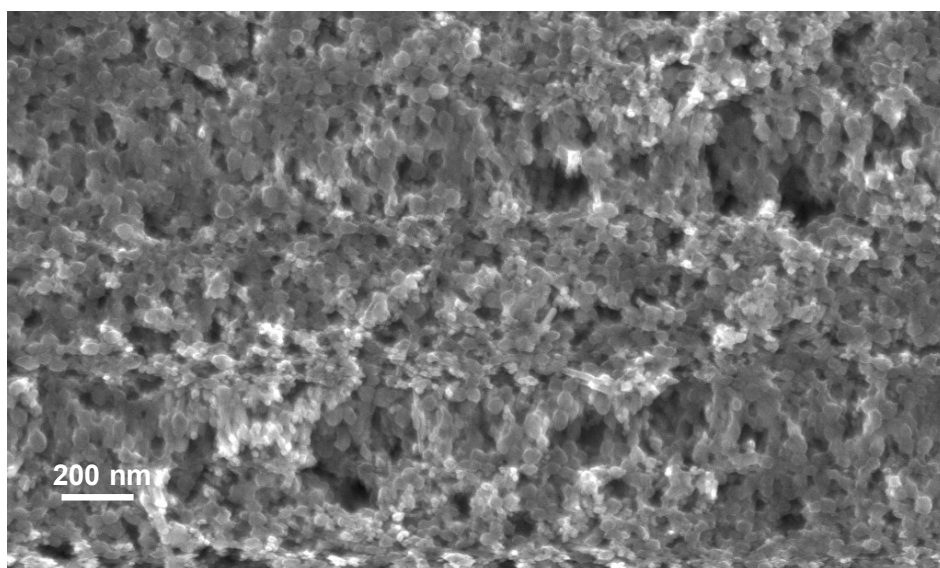
Max DeMarco¹, Matthew Ballard¹, Elinor Grage¹, Farnoush Nourigheimasi¹, Lillian Getter¹, Ashkan Shafiee^{2,3}, and Elham Ghadiri^{1,2,3*}

1. Chemistry Department, Wake Forest University
2. Wake Forest School of Medicine, Wake Forest University
3. Center for Functional Materials, Wake Forest University

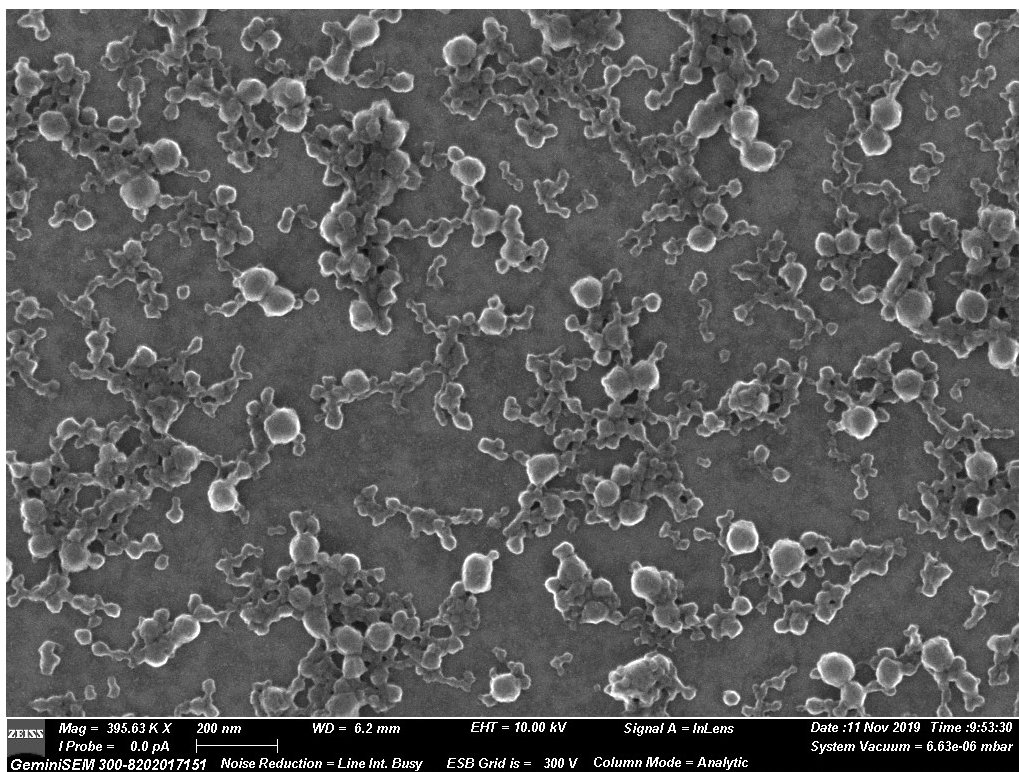
* Author to whom any correspondence should be addressed. ghadire@wfu.edu



Supplementary Figure S1. Example of dopamelanin films prepared by drop-casting. Controlling the film's uniformity is difficult with this method.



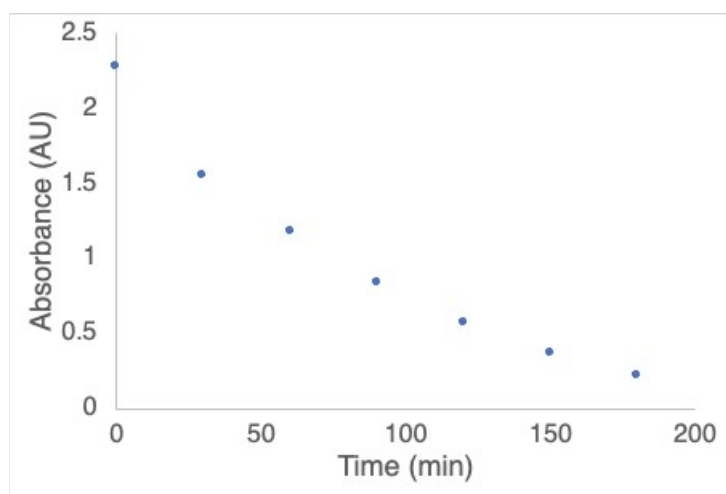
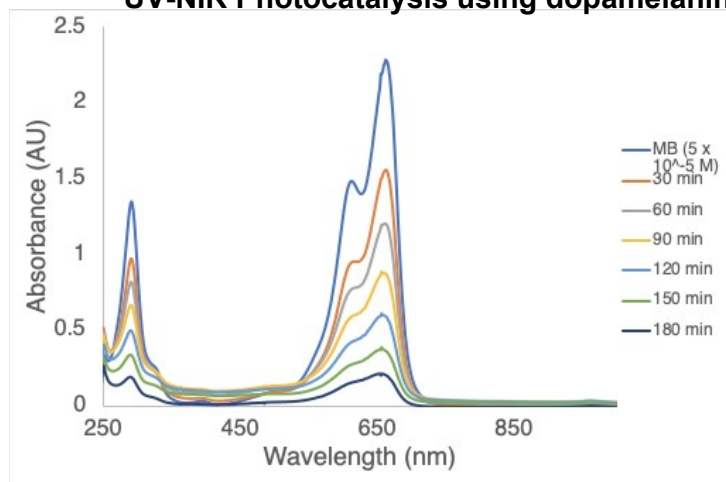
Supplementary Figure S2. SEM image of a mesoporous TiO₂ film. Particle size is about 20-40 nm.

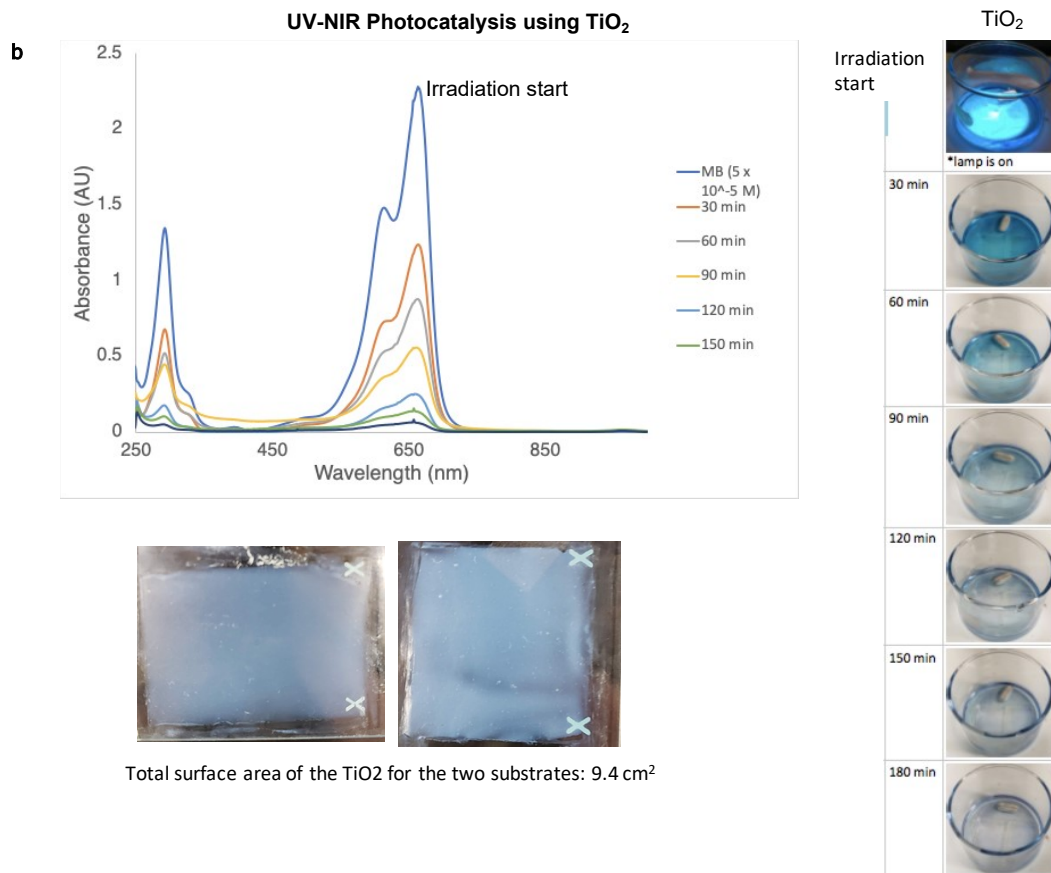


Supplementary Figure S3. SEM Image of synthetic melanin. Temperature fluctuation during synthesis results in random polymerization of monomeric units and random morphology.

Details of photocatalysis measurements. Results shown in the main manuscript and Figures S4 and S5 represent several iterations and control tests.

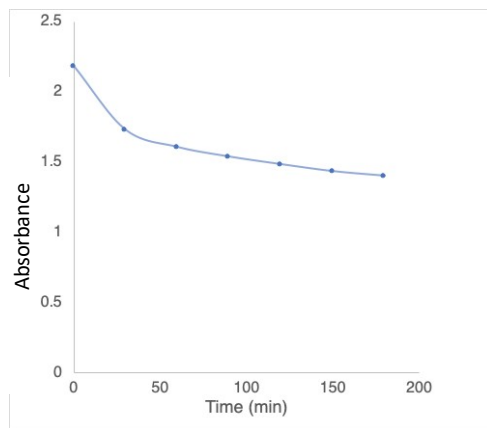
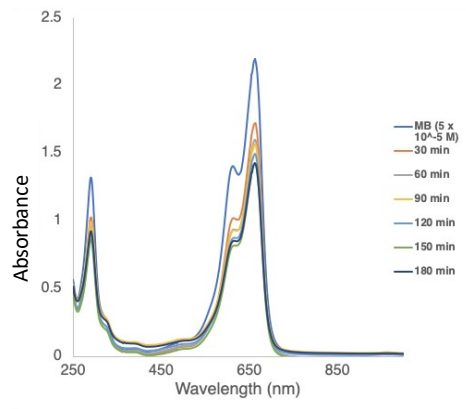
a UV-NIR Photocatalysis using dopamelanin-TiO₂

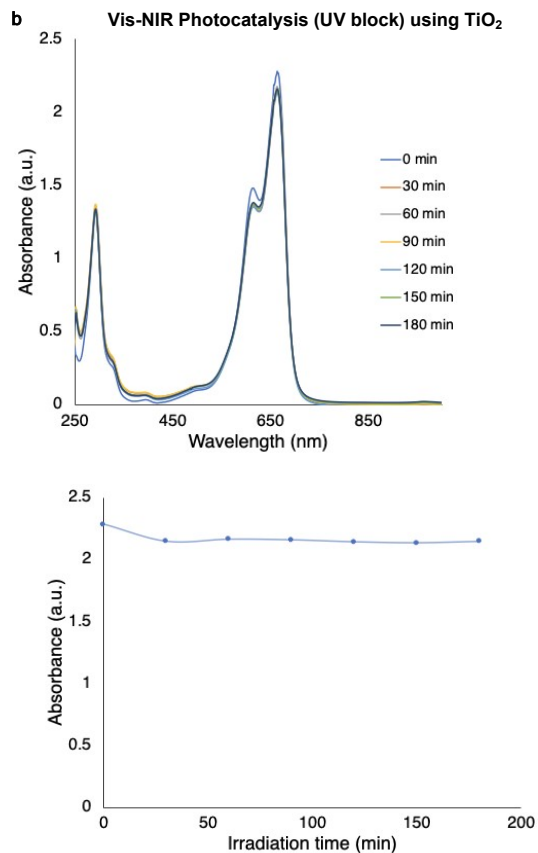




Supplementary Figure S4. Details of photocatalysis measurements using dopamelanin-TiO₂ and TiO₂ films under UV-NIR irradiation. The total macroscopic film area is 9.4 cm². Figures 3a,b in the manuscript show the results.

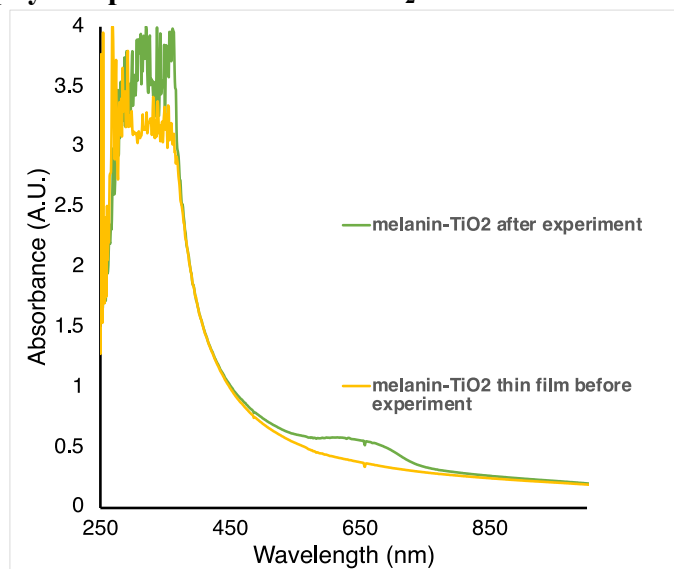
a Vis-NIR Photocatalysis (UV block) using dopamelanin-TiO₂





Supplementary Figure S5. Vis-NIR (UV Block) irradiation of dopamelanin-TiO₂ and TiO₂ thin film. Figure 3c in the manuscript shows the results.

The amount of MB physisorption on melanin-TiO₂

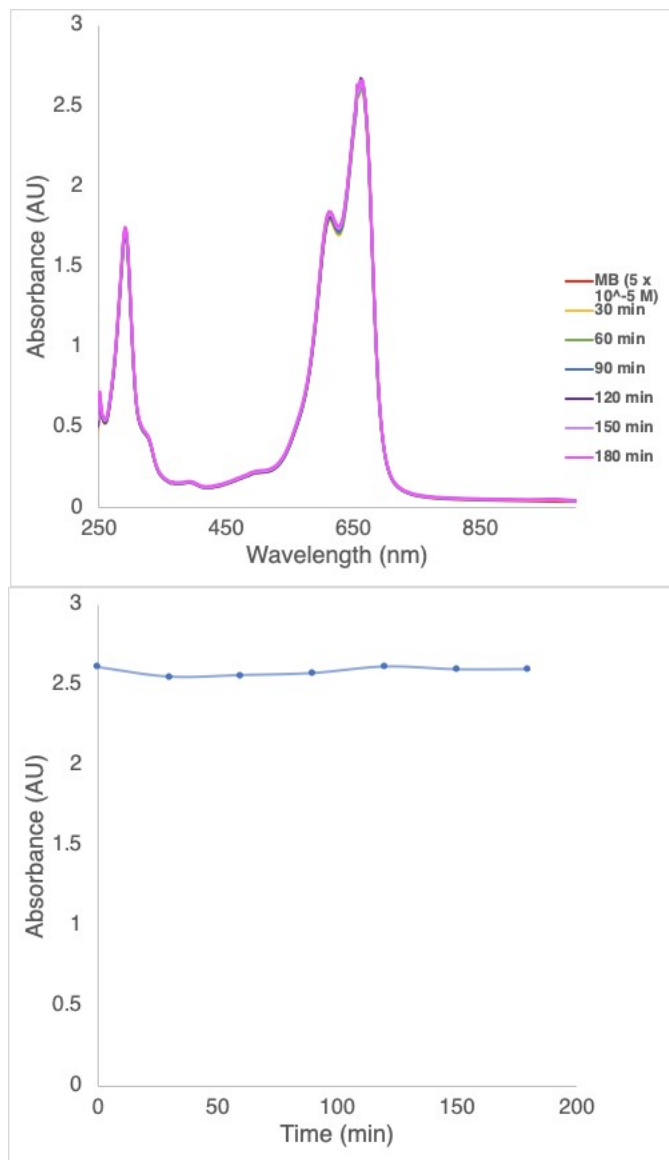


Supplementary Figure S6. The optical absorption of the dopamelanin-TiO₂ film before and after photocatalytic removal of MB. The peak at 650 nm reflects the amount of MB adsorbed

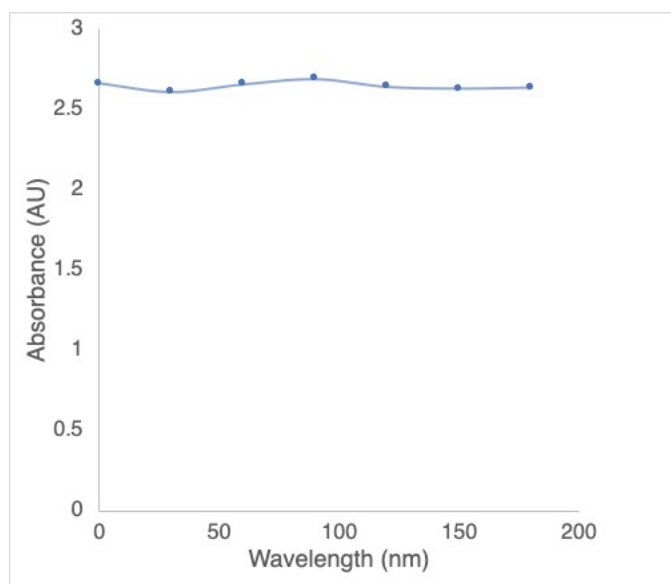
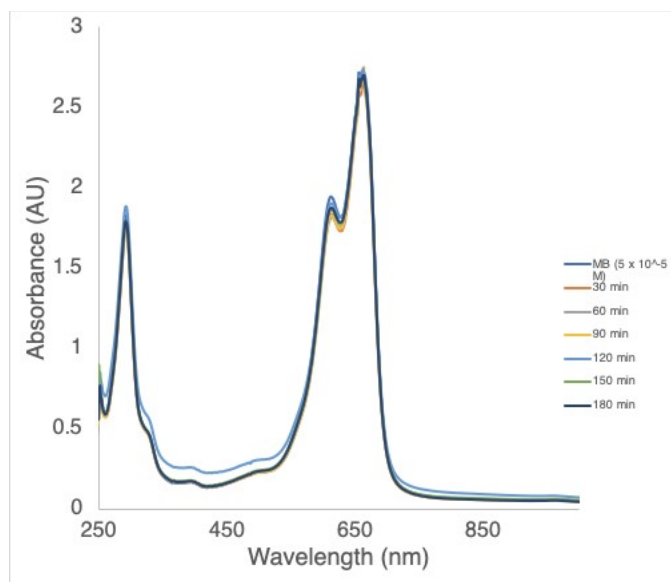
on the surface of dopamelanin-TiO₂ film. The absorption change of 0.1 indicates that the concentration change due to adsorption is marginal compared to the photocatalytic removal of MB shown in photocatalysis tests.

Control photochemical experiments under dark.

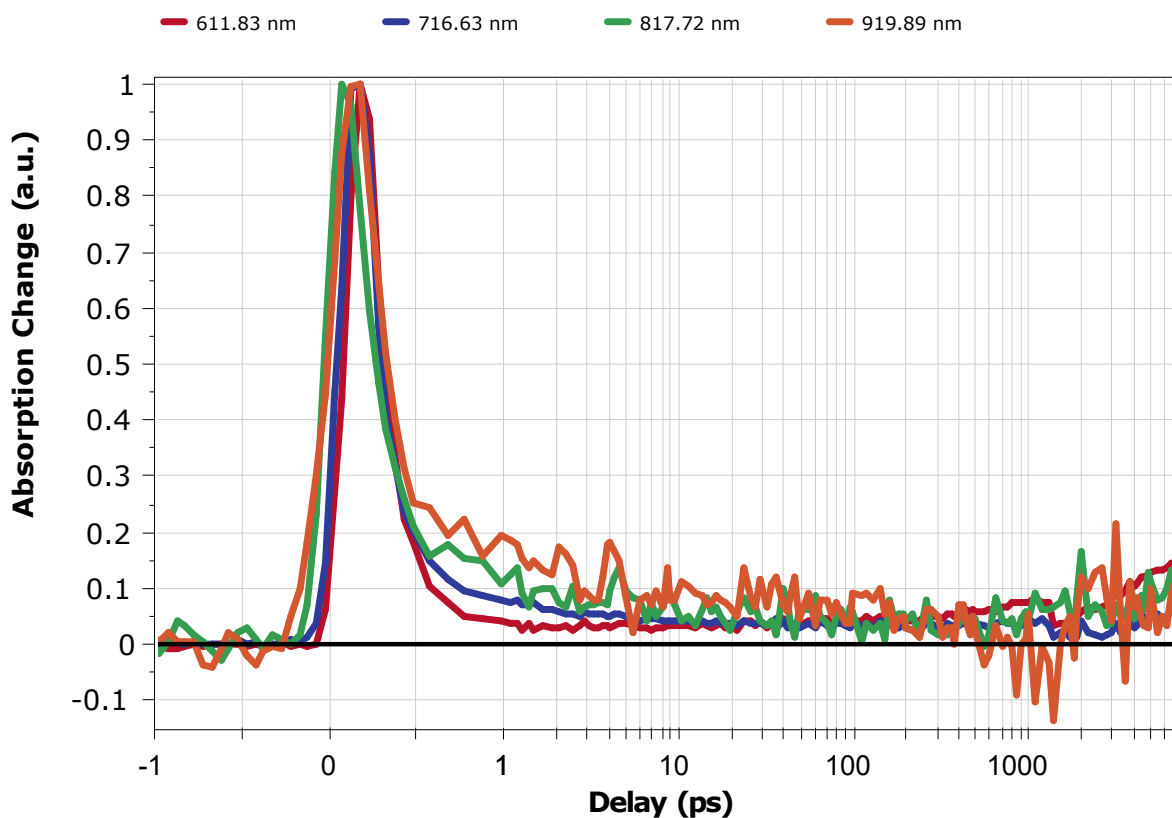
In control experiments, melanin-TiO₂ and TiO₂ thin films were immersed in MB solution under dark conditions, and MB absorption was measured at the specified time intervals.



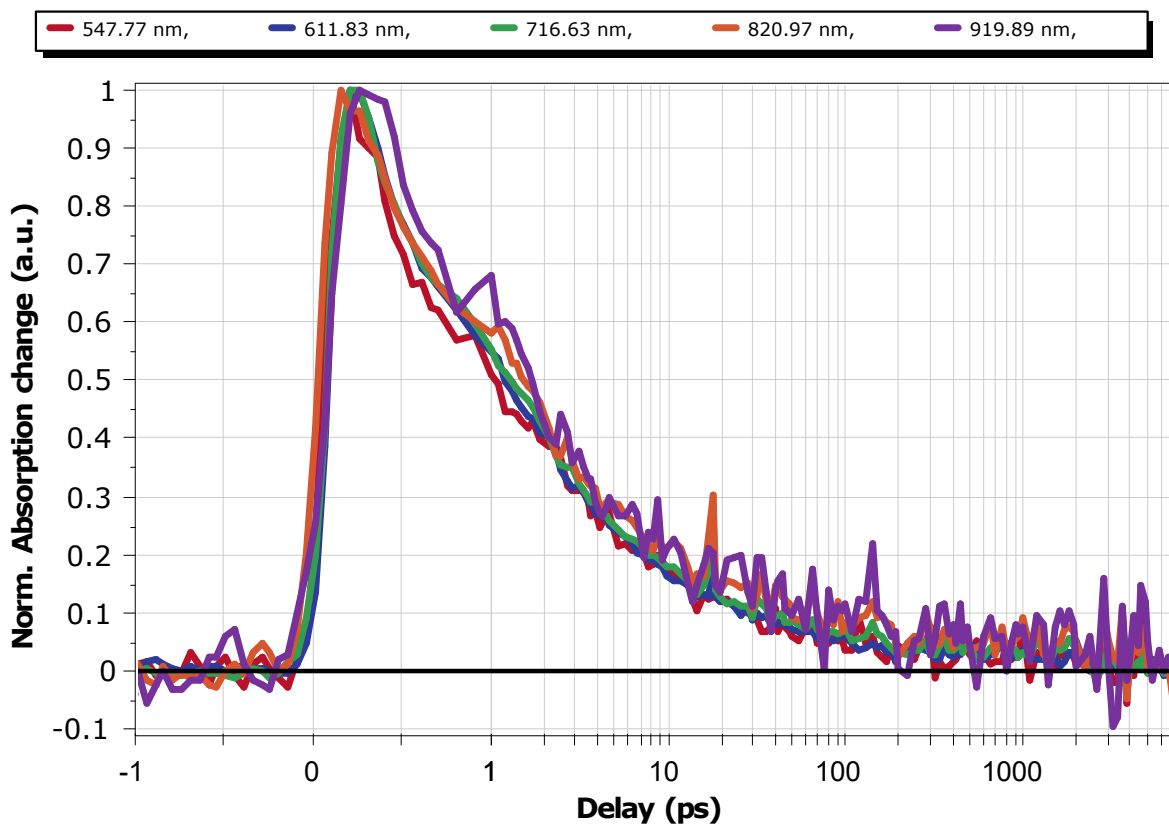
Supplementary Figure S7. Control catalysis tests on TiO₂ film under dark conditions (no irradiation). No MB decomposition is observed.



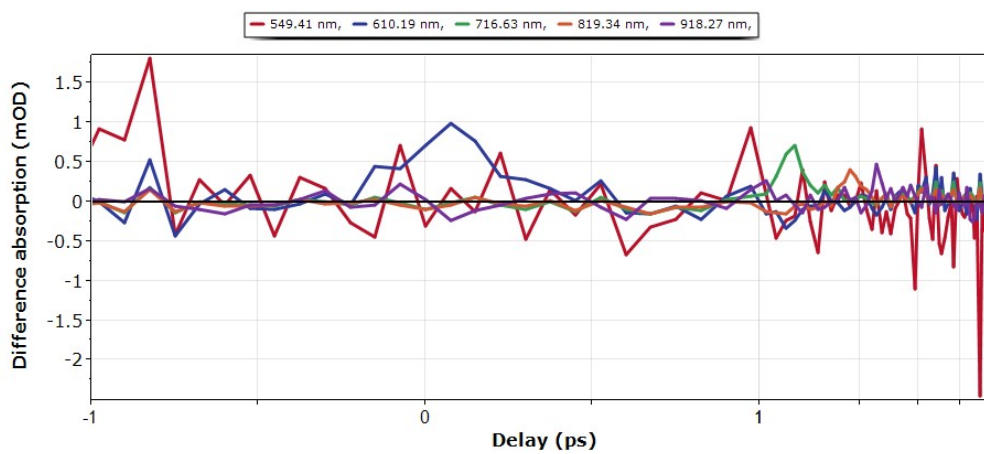
Supplementary Figure S8. Control catalysis tests on dopamelanin-TiO₂ film under dark conditions (no irradiation). No MB decomposition is observed.



Supplementary Figure S9. Normalized transient absorption signal of melanin sample. The relaxation of the signals occurs in less than 10 ps. The ultrafast excited state relaxation in synthetic melanin nanoparticles measured with broadband TAS agrees with previous reports of melanin nanoparticles using two-color pump probe spectroscopy and time resolved photoluminescence of melanin (oligomers and polymers) as discussed in manuscript section 3.6.

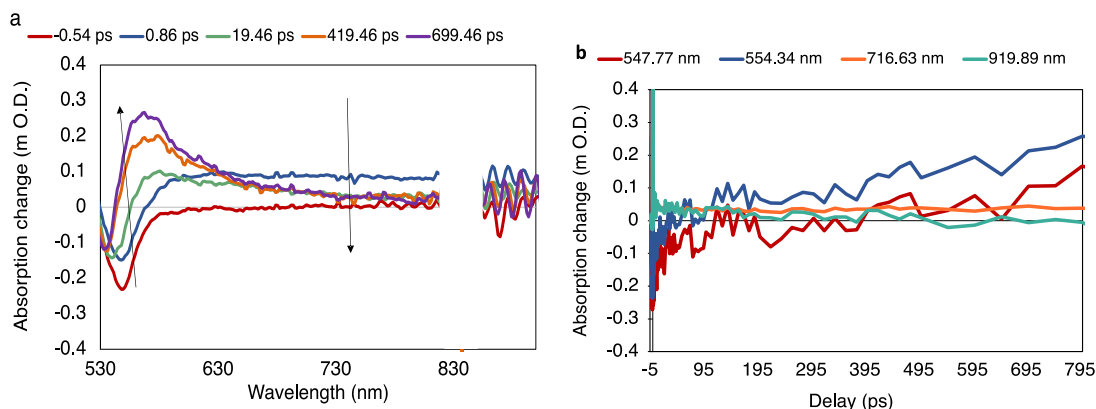


Supplementary Figure S10. Normalized transient absorption signal of melanin sample. The relaxation of the signals occurs in less than 10 ps.

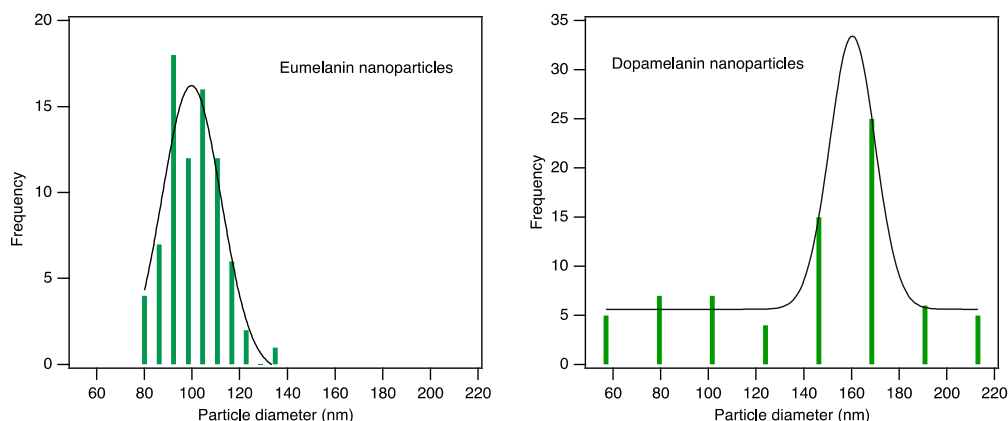


Supplementary Figure S11. Transient absorption measurement on TiO₂ mesoporous film with a 460 nm pump. The experimental parameters are similar to those for the melanin-TiO₂ sample. No transient absorption signal was observed with 460-nm excitation since TiO₂ does not

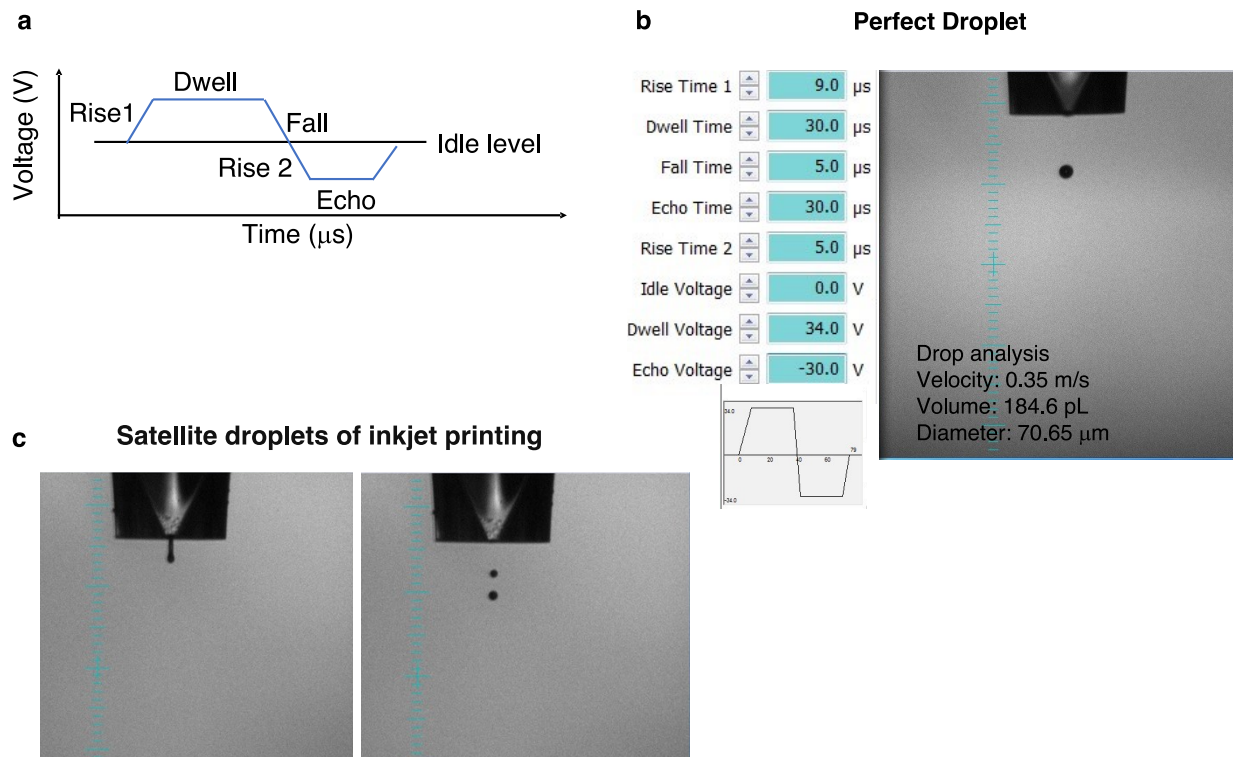
absorb the pump beam. These data serve as a baseline measurement for the TAS experiments performed on the melanin-TiO₂ sample. For the melanin-TiO₂ sample, the 460 nm directly excites melanin, and the TAS signal represents the photoexcited dynamics of charge carriers in melanin and/or injected into TiO₂ (melanin as sensitizer).



Supplementary Figure S12. The broadband spectrum and the long scan time traces of melanin films.



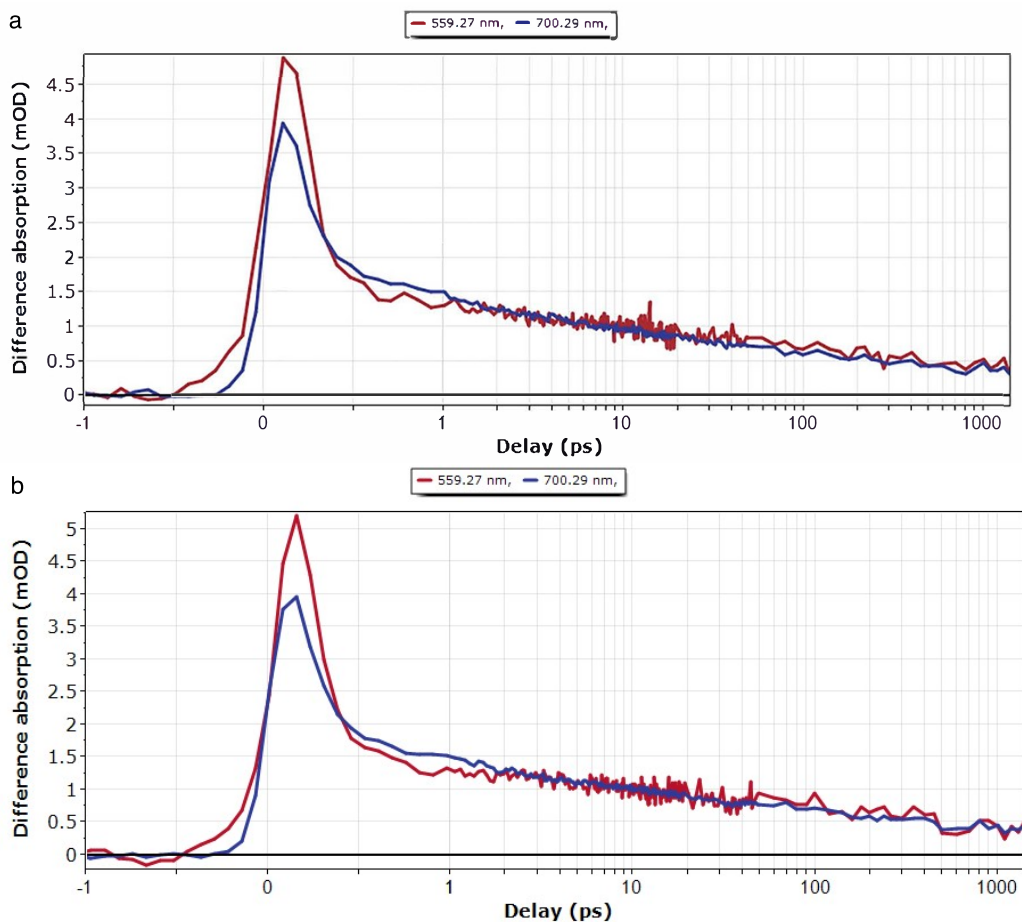
Supplementary Figure S13. Size distribution analysis of melanin nanoparticles. The analysis is performed on the SEM images shown in Figures 1a and 1b of the main text. The center of gaussian fit to the data shows 100 nm for eumelanin nanoparticles and 160 nm for dopamelanin nanoparticles.



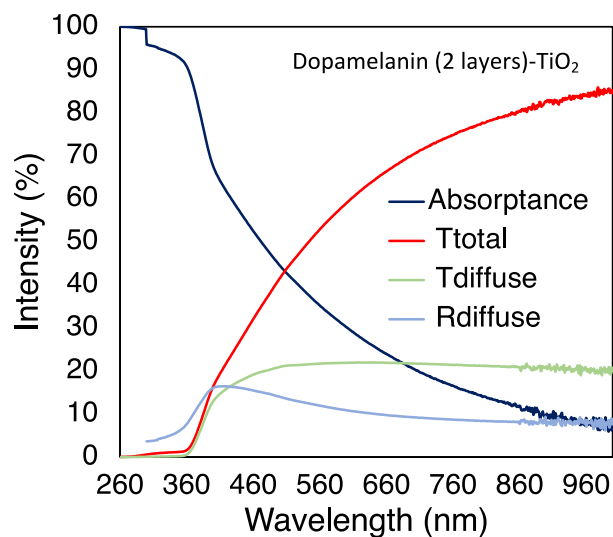
Supplementary Figure S14. Inkjet printing parameters. a) The shape of the Bipolar waveform to inkjet print functional materials. b) Bipolar waveform shape parameters and image of a desired droplet used for printing. The drop analysis parameters are defined as velocity 0.35 m/s, volume 185 pL and drop diameter 70.65 μm. c) an example of a non-ideal printing. The satellite formation and consequently the daughter drop (a smaller droplet with a lower speed) impact on thin film quality.

Photostability tests.

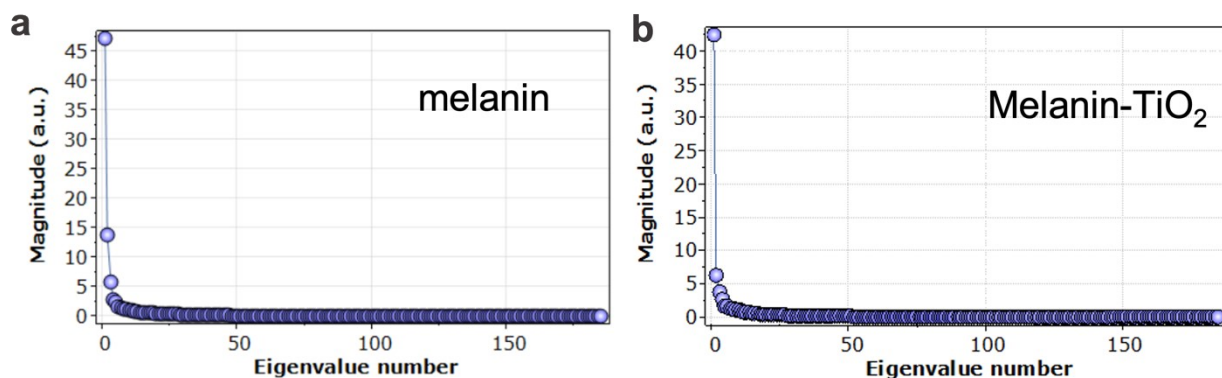
An example control test at much higher power (compared to what is reported in manuscript) is provided and added to the manuscript.



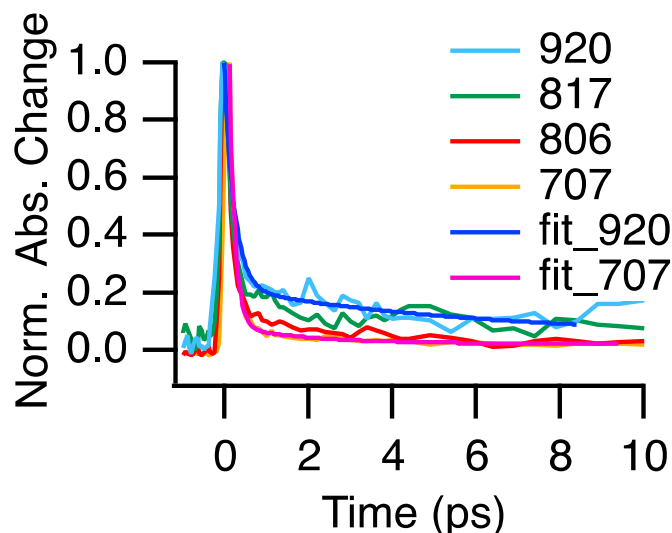
Supplementary Figure S15. a,b) Two consecutive measurements of melanin/TiO₂ sample. Excitation is at 460 nm. Probe is white light (WL). The signal amplitude and kinetics is reproduced. The pump power is 5.5 mW and the WL probe power is 558 μ W (measured at 715 nm). This experiment shows the sample is stable at such high power. The experiments shown in the manuscript are performed at much lower power (pump 460 μ W).



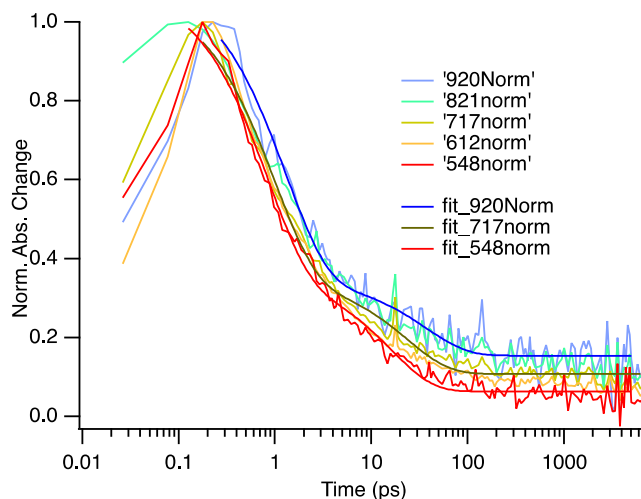
Supplementary Figure S16. The optical characteristics of Dopamelanin (2 layers)-TiO₂ film. The diffuse transmission and diffuse reflection components are having much smaller contributions compared to direct transmission. The sharp absorption edge at 380 nm belongs to TiO₂ bandgap and the broad absorption in Vis-NIR is due to absorption by melanin.



Supplementary Figure S17. The magnitude of components of SVD analysis. The first three components are the most significant for analysis of data matrix. The temporal-wise and Wavelength-wise of these three components are provided in the manuscript.



Supplementary Figure S18. Short-time-delayed TAS signal of melanin nanoparticles at different probe Wavelengths in NIR. The time-traces at 707 nm and 920 nm are fitted with double exponential function. The magenta and blue traces are the fit to the TAS at 707 nm and 920 nm respectively. The fit parameters for 920 nm-probe are ($A1 = 0.168$, $\tau1 = 5.99$ ps, $A2 = 0.730$, $\tau2 = 0.239$ ps and $y0 = 0.05$) and for 707 nm-probe are ($A1 = 0.065$, $\tau1 = 1.9$ ps, $A2 = 1.94$, $\tau2 = 0.135$ ps and $y0 = 0.024$). The $\tau2$ values are within the time-resolution of the TAS experiment ~ 350 fs. The $\tau1$ values reflect the ESA relaxation time constant of melanin being 5.99 ps and 1.9 ps recorded at 920 nm and 707 nm.



Supplementary Figure S19. Normalized time-delayed TAS signal of melanin-TiO₂ at different probe Wavelengths in Vis and NIR and double exponential fitting traces. The time-traces at 548 nm, 717 nm, and 920 nm are fitted with double exponential function. The fit parameters for 920 nm-probe are ($A1 = 0.19263$, $\tau1 = 36.3$ ps, $A2 = 0.75663$, $\tau2 = 1.28$ ps and $y0 = 0.15428$). The fit parameters for 717 nm-probe are ($A1 = 0.23881$, $\tau1 = 23.44$ ps, $A2 = 0.72454$,

$\tau_2 = 0.968$ ps and $y_0 = 0.10804$). The fit parameters for 548 nm-probe are ($A_1 = 0.28886$, $\tau_1 = 15.94$ ps, $A_2 = 0.74$, $\tau_2 = 0.818$ ps and $y_0 = 0.063429$).

$$y = y_0 + A_1 \exp - \text{inv} \tau_1 \cdot t + A_2 \exp - \text{inv} \tau_2 \cdot t$$

Equation S1